Int J Adv Life Sci Res. Volume 9(4) 193-205
https://doi.org/10.31632/ijalsr.2026.v09i04.012

International Journal of Advancement in Life Sciences Research

Online ISSN: 2581-4877

Journal homepage http://ijalsr.org



Original Article

Phlorizin from *Bauhinia blakeana* Leaves: Isolation, HDAC8 Docking Analysis, Cytotoxicity in SH-SY5Y Neuronal Cells, and Implications for Alzheimer's Disease

Kalaiselvi Chinnamuthu, Saravanan Gopal*

Department of Pharmaceutics, Faculty of Pharmacy, Karpagam Academy of Higher Education, Eachanari, Seerapalayam, 641021 Tamil Nadu, India

Corresponding Author's Email: saravananpharma26@gmail.com

Abstract

Bauhinia blakeana leaves, an understudied medicinal plant, harbor phlorizin (PZ), a natural dihydrochalcone with antioxidant properties that might play into Alzheimer's disease pathways through glucose handling and inflammation control. This work set out to isolate PZ from *B. blakeana* leaves, verify its structure, test its effects on neuron-like SH-SY5Y cells, and check how it binds to HDAC8, a key epigenetic target in neurodegeneration via computational docking. PZ came out clean from silica gel chromatography (fractions 54-62, single TLC spot at Rf 0.38), confirmed by melting point 110-113°C, ESI-MS m/z 437.2 [M+H]+, diagnostic NMR peaks for aromatic/sugar protons and carbons, and FTIR for OH/CO groups. PZ docked solidly into HDAC8's active site (-4.79 kcal/mol binding energy, Ki 7.28 μM), held by H-bonds to His143 (2.8 Å), His180 (2.9 Å), and Gly206 (2.7-3.1 Å), and hydrophobic fits with Phe207/Tyr306. In cells, it slashed viability dose-dependently, down to 8% at 40 μg/mL, IC50 9.13 μg/mL, with neurites retracting and cells shrinking above 10 μg/mL. This study showed that *Bauhinia blakeana* leaves were a reliable source of phlorizin and that the isolated compound was structurally identical to PZ reported from other plants. Computational docking suggested that phlorizin can occupy the catalytic pocket of HDAC8 in a reasonable binding orientation, pointing to a potential interaction with epigenetic machinery. In differentiated SH-SY5Y cells, phlorizin produced a clear, concentration-dependent loss of viability that matched the observed morphological damage.

Keywords: *FTIR; HDAC8; MTT assay; Phlorizin; SH-SY5Y*

Introduction

Alzheimer's disease (AD) is a neurological ailment that worsens with age and progressively erodes memory, thinking ability, and independence and is ultimately fatal (Scheltens *et al*., 2021). It accounts for the majority of dementia cases in older adults and, with aging populations, has become a major medical, social, and economic challenge worldwide. Current pharmacological treatments offer only modest symptomatic benefit and have little impact on the underlying disease course, underscoring the need for new therapies that target core pathogenic mechanisms (Long & Holtzman, 2019).

Natural products have attracted growing interest as potential modulators of neurodegenerative processes, including those involved in AD. Traditional medicinal systems have been used for centuries to support memory and treat age-related cognitive decline, and a number of these traditional preparations are now being investigated using modern experimental approaches (Solanki *et al*., 2015). Many plant-derived compounds, particularly phenolics and flavonoids, display a combination of antioxidant, anti-inflammatory, and anti-apoptotic actions, can chelate redox-active metals, and influence signalling pathways that regulate neuronal survival, synaptic plasticity and mitochondrial function (Williams & Spencer, 2012). Such multitarget properties are particularly desirable in AD,

Received on :15th April 2026; Revised version received on :21st September 2026; Accepted:29th September 2026

where multiple pathological mechanisms operate simultaneously and may require combination or pleiotropic approaches rather than single-target strategies (Cavalli *et al*., 2008).

Bauhinia blakeana is an ornamental and ethnomedicinal plant, but its phytochemical profile and pharmacological activities remain relatively underexplored compared to other species of the genus. Preliminary reports on Bauhinia species have revealed the presence of flavonoids, glycosides, tannins, and other bioactive constituents with antioxidant, antimicrobial, and anti-diabetic properties, suggesting that *B. blakeana* may also harbor biologically significant molecules with potential neuroprotective effects (Rajani & Kanaki, 2008).

Phlorizin (PZ) is a dihydrochalcone glycoside that was first reported from apple bark and leaves and has since been identified in several plant species (Ehrenkranz *et al*., 2005; Gosch *et al.,* 2010). In the present study, PZ is isolated from *B. blakeana*, adding this species to the list of natural sources of the compound. To the best of our understanding, this is the first report of PZ being isolated from *B. blakeana* and evaluated for anti-Alzheimer's activity in SH-SY5Y cells, along with its in-silico interaction with the Alzheimer's-related protein 5VI6. It is well known as a natural inhibitor of sodium-glucose co-transporters (SGLT1 and SGLT2) (Rieg & Vallon, 2018). Beyond its classical role as a prototype SGLT inhibitor and its relevance to glucose homeostasis and diabetes research, researchers have increasingly focused on PZ's diverse bioactivity, which extends to potent antioxidant, anti-inflammatory, and anti-glycation effects (Najafian *et al*., 2012). Experimental studies have shown that PZ and related dihydrochalcones can mitigate oxidative stress, regulate mitochondrial function, and safeguard cells against toxin or Aβ-induced damage, thereby supporting their potential as neuroprotective agents (Chhimwal *et al*., 2022). Its ability to interfere with pathways implicated in insulin resistance and metabolic dysfunction may also be relevant to AD, which is sometimes described as a "type 3 diabetes" due to shared pathogenic mechanisms.

However, there is a paucity of information on the occurrence of PZ in *B. blakeana* and, to date, no detailed account of its isolation from this species coupled with comprehensive spectroscopic characterization and functional evaluation in neuronal cell models of AD. Moreover, while several in-silico studies have examined the interaction of natural compounds with various AD-related targets, the specific molecular interaction of PZ with the crystal structure of histone deacetylase 8 in complex with trapoxin A. Addressing these gaps, the present study focuses on the isolation of PZ from *B. blakeana*, its structural confirmation using 1H-NMR, 13C-NMR, FTIR, and mass spectrometry, the assessment of its anti-Alzheimer's activity in SH-SY5Y neuroblastoma cells, and the in-silico evaluation of its binding affinity and interaction profile with 5VI6 protein structure. This study aims to illuminate PZ's neurotherapeutic potential and broaden the pharmacological significance of *B. blakeana* as a source of bioactive compounds for AD research by integrating in vitro, computational, and phytochemical methods.

Materials and Methods

Plant Collection and Identification

Whole plant material of *B. blakeana* was collected from Sankari village, Salem district, Tamil Nadu, India and was confirmed by a scientist at the Ministry of Environment, Forest & Climate Change, with voucher specimen number BSI/SRC/5/23/2022/TECH/608. The collected plant parts were carefully washed to remove surface dirt and debris, then dried at a controlled room temperature (28 ± 2°C) in the shade for 10-15 days until they reached a constant weight. The dried material was coarsely powdered using a mechanical grinder (40-60 mesh size) and kept in sealed containers under refrigerated conditions (4°C) until further extraction was carried out. The whole plant was utilized based on its traditional medicinal uses and documented pharmacological significance.

Isolation

After dissolution in methanol, the crude extract was blended with silica gel (60-120 mesh) to ensure uniform adsorption. The subsequent dried powder was applied to a Merck silica gel column (100-200

mesh) previously prepared using petroleum ether. Elution was first carried out with hexane, followed by a gradient of hexane:ethyl acetate mixtures (90:10, 80:20, 70:30, 60:40, 50:50, 40:60, 30:70, 20:80, 10:90) and then 100% ethyl acetate, as summarized in Table 1. The column was further eluted with ethyl acetate: chloroform (90:10, 80:20, 70:30, 60:40, 50:50, 40:60, 30:70, 20:80, 10:90) and 100% chloroform.

Table 1: *Column Chromatography Fractions of the Crude Extract with Corresponding Solvent Systems*

Sl. No.	Fractions	Solvent System & Ratios
1	F-1	Hexane. (100%)
2	F-2 to F-28	Hexane: et. acetate (90:10 → 10:90)
3	F-29	Et. acetate (100%)
4	F-30 to F-43	Et. acetate: Chloroform. (90:10 → 10:90)
5	F-44	Chloroform (100%)
6	F-45 to F-53	Chloroform: MeOH (99:1; 98:2; 97:3)
7	F-54-F-62	Chloroform: MeOH (96:4; 95:5)
8	F-63 to F-68	Chloroform: MeOH (94:6; 92:8; 90:10; 88:12; 85:15; 80:20)

Spectroscopic Analyses

A SERVO melting point apparatus (uncorrected) was used to test the melting point in open glass capillaries. For structural characterization, 1H and 13C NMR spectra were acquired via a JEOL spectrometer operating at 500 MHz and 125 MHz, respectively. A high-resolution mass spectrum was obtained using a JEOL AccuTOF JMS-T100LC instrument in ESI positive mode with a capillary voltage of 3.2 kV.

In Silico Molecular Docking Analysis

Software Used

AutoDock 4.2, Avogadro Tools, and Discovery Studio Visualizer were employed for docking studies (Morris *et al*., 2009; Kim *et al*., 2021).

Protein Selection

Human histone deacetylase 8 (HDAC8) served as the target protein. Its crystal structure (PDB ID: 5VI6) was retrieved from the RCSB Protein Data Bank (Banerjee *et al*., 2019).

Protein and Ligand Preparation

All crystallographic water molecules were removed from the HDAC8 structure to prevent interference at the docking site and to maintain consistency. Co-crystallised ligands, cofactors, and non-essential heteroatoms (except essential structural ions) were also deleted, retaining only the apo form of the protein for docking. The 2D structure of PZ was sourced from the PubChem database and energy-minimised using the GAFF force field in Avogadro Tools (Hanwell *et al*., 2012).

Molecular Docking Protocol

Molecular docking of PZ with HDAC8 was carried out using AutoDock 4.2. Polar hydrogen atoms were incorporated into the receptor structure, and Kollman charges were assigned accordingly. The ligand molecule was prepared by specifying its rotatable bonds before docking analysis. The binding pocket was specified using literature-reported coordinates, and a grid box centered on the orthosteric site was generated (50 × 50 × 50 points, grid spacing of 0.375 Å) to cover a region of 5 Å around the active site. All docking settings were maintained at the standard default configuration, with the exception of the genetic algorithm (GA) runs, which were set to 100 to enhance conformational sampling (Trott & Olson, 2010, Ribeiro *et al*., 2018). The resulting docking poses were clustered and ranked according to their binding energies. The most favorable conformation was chosen based on its lowest binding energy and key hydrogen-bond interactions within the top-ranked clusters. Ligand-

receptor interactions and binding affinities were examined and visualized using Discovery Studio Visualizer.

Cytotoxicity Study

Cell Line and Differentiation

Following retinoic acid-induced neuronal development, the cytotoxicity of PZ was assessed using SH-SY5Y cells which exhibit neuronal properties when differentiated, making them suitable for assessing neurotoxicity (Xicoy*et al*., 2017).

Cell Culture and Differentiation

Following a 24 h incubation period to facilitate cellular attachment, the growth medium was replaced with a differentiation-inducing medium containing 10 µM all-trans retinoic acid (ATRA) and a reduced serum concentration (1-2% FBS). Cells were maintained for 5 days with daily medium changes to induce neuronal differentiation (Encinas *et al*., 2000; Cheung *et al*., 2009).

MTT Assay

On day 6, differentiated PZ at concentrations of 2.5-40 µg/mL in differentiation medium for 24-48 hours. Then, cell viability was evaluated, followed by an incubation period of 3-4 h at 37°C (Mosmann, 1983). After, utilizing 630 nm as the reference wavelength, net absorbance values were obtained by subtracting the 630 nm background, and the percentage of viable cells was normalized against the vehicle-treated control group according to the following equation:

% Cell viability = [(A570 treated - A630 treated)/(A570 control - A630 control)] x 100

Dose-response curves were plotted with % viability (Y-axis) versus log[phlorizin] (µg/mL, X-axis). IC_{50} values were determined using non-linear regression in GraphPad Prism-8 from three independent experiments (mean ± SD).

Results

Isolation of Chemical Constituents

Column chromatography of the extract of *B. blakeana* leaves, after pre-adsorption onto silica gel (60-120 mesh), yielded 68 fractions of 100 mL each (Table 1). TLC analysis using chloroform: methanol (90:10) revealed that fractions 54-62 contained a single spot with an Rf value of 0.38, corresponding to the isolated compound PZ as shown in Table 2. The relevant fractions were pooled to yield a crude solid. This material was subsequently purified by treatment with activated charcoal in hot ethanol, followed by crystallization, obtaining pure PZ as a white amorphous powder.

Table 2: *Thin-Layer Chromatographic Analysis of Isolated Phlorizin*

Isolated Compound	TLC Solvent System	No of Spots	Rf Value
Phlorizin	Chloroform:methanol (90:10)	1	0.38

Spectral Characterisation of Phlorizin

As shown in Figure 1, detected a molecular ion peak at m/z 437.2, C21H24O10. The isolated product was produced as an off-white solid, m.p. 110-113°C.

As shown in Figure 2 displayed characteristic signals including three aromatic hydroxyl protons at δ 13.51 and 9.10 (s, 1H, 4-OH). Aromatic protons appeared as doublets at δ 7.02 and δ 6.63-6.65, along with δ 6.12 (d, 1H, H-3) and δ 5.93 (d, 1H, H-5). Anomeric proton was observed at δ 5.05-5.07 (d, 1H, H-1''), with sugar protons in the region δ 3.17-3.73 (m) and methylene protons at δ 2.76-2.80 (t, 2H, H-1β). Additional signals included hydroxyl protons at δ 4.59-4.62 (t, 1H, 6''-OH) and δ 4.92-5.31 (4H, sugar OH).

As shown, it exhibited 24 carbon signals: δ 204.71 (C=O), 165.38 (C-4'), 164.43 (C-6'), 160.83 (C-2'), 155.27, 114.97 (C-6), 105.12 (C-3), 100.78 (C-5), 96.79 (C-1''), 94.29 (C-1'), 77.26 (C-3''), 76.66 (C-5''), 73.18 (C-4''), 69.39 (C-3''), 60.51 (C-2''), 44.97 (C-1α), 28.99 (C-1β).

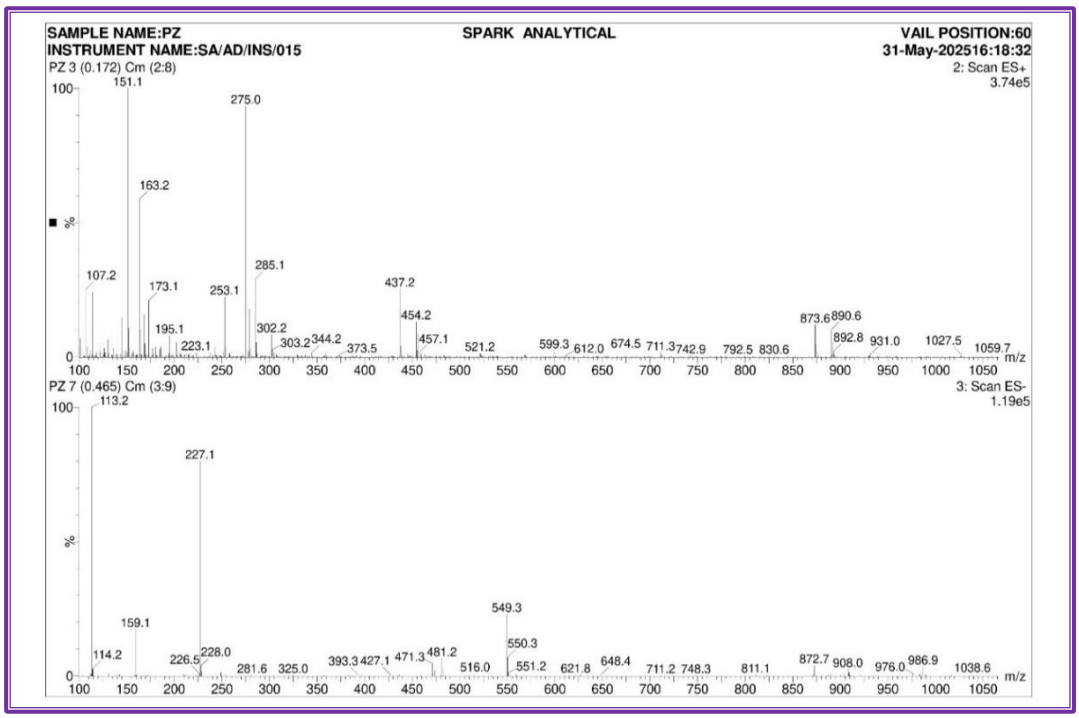


***Figure 1**: Mass Spectrum of Phlorizin Showing the Molecular Ion At M/Z 437.2 [M+H]* $^{+}$

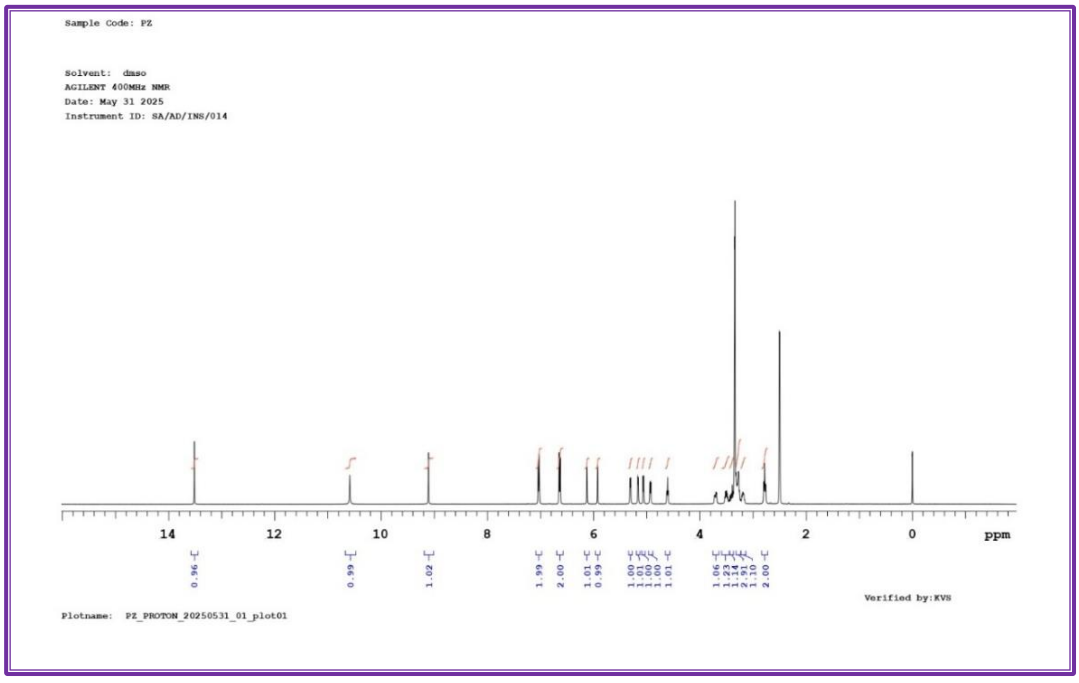


***Figure 2:** 1H-NMR spectrum of Phlorizin*

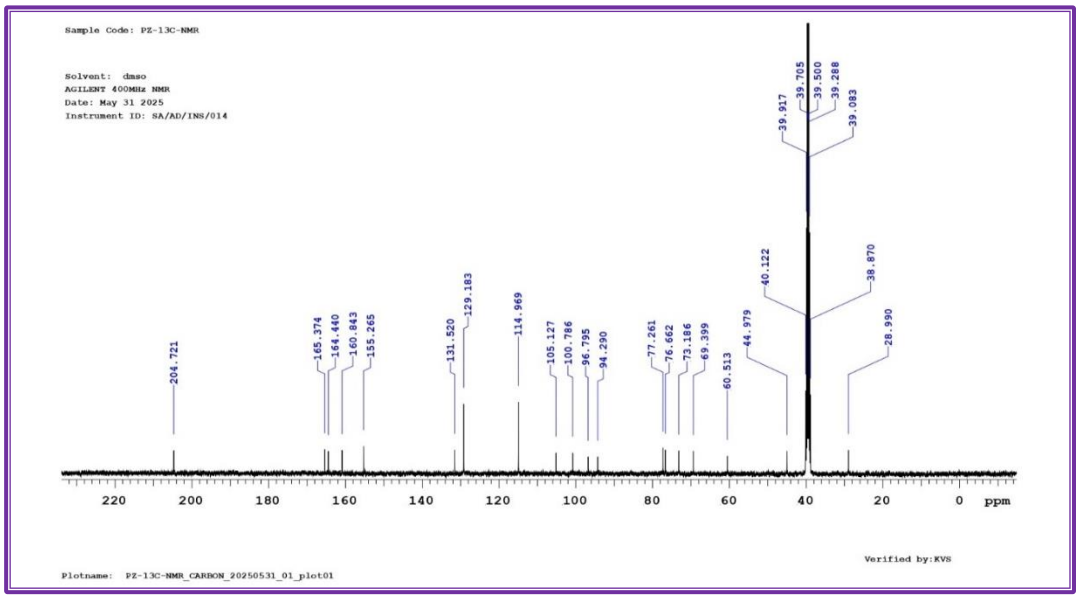


Figure 3: *13C-NMR Spectrum of Phlorizin*

FT-IR (KBr) showed absorption bands at 3522, 3360 (O), 2933, 2889, 1463 as shown in Figure 4. All spectral data were in complete agreement with reported values for PZ(Perumal *et al.,* 2023).

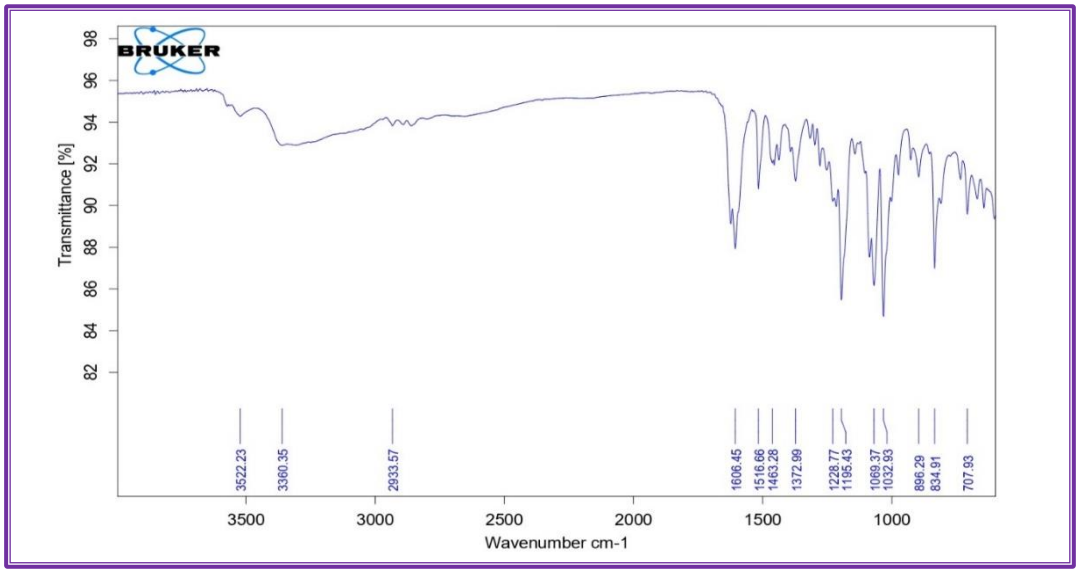


Figure 4: *FT-IR Spectrum of Phlorizin (KBr pellet)*

In Silico Analysis

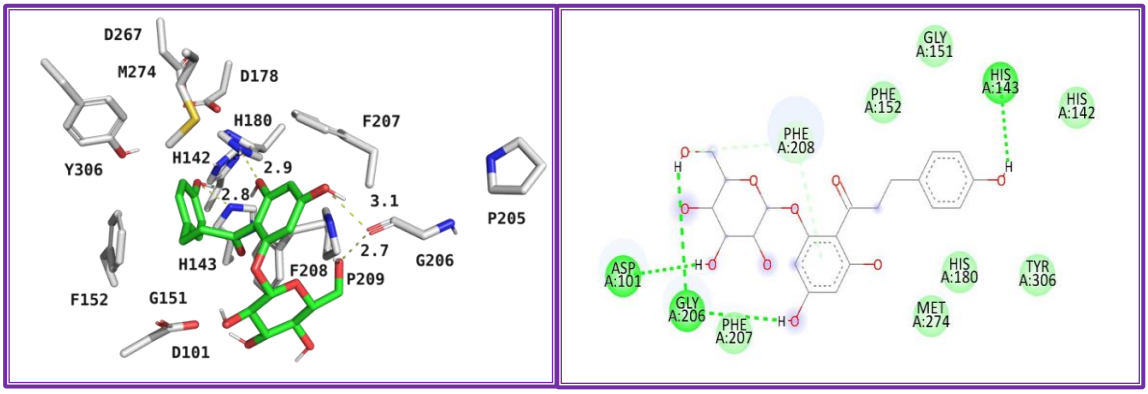
Docking analysis on 5VI6

Examine the binding of PZ to human histone deacetylase 8 (HDAC8, PDB ID: 5VI6). Molecular docking analysis showed that PZ bound to HDAC8, having a modest affinity for the target protein.

The docked pose showed that PZ is stabilized in the catalytic pocket by multiple hydrogen bonds with key residues. Hydrogen bond contacts were observed with His143, His180, and Gly206, with distances in the range of 2.7-3.1 Å, positioning the ligand deep within the active-site region. Additional contacts with surrounding residues such as Asp101, Gly151, Phe208, Phe207, Met274, Tyr306, and others further contribute to the overall stabilization of the complex (Vannini *et al.,* 2007), as illustrated in the 3D and 2D interaction diagrams (Figure 5a, b). These interactions support a favorable binding orientation of PZ within HDAC8 and are consistent with its predicted inhibitory potential.

Table 3: *Binding Energy and Predicted Inhibition Constants of Phytocompounds Against Protein Target*

Compound	Protein	Binding Energy (kcal/mol)	Predicted Inhibition Constant	Hydrogen Bond Distance (Å)
Phlorizin	Human histone deacetylase 8	-4.79	07.28 µM	His143 (2.8Å), His180 (2.9Å), Gly206 (3.1Å), Gly206 (2.7Å)



a b

Figure 5 a and b*: 3D And 2D Interaction Between Phlorizin and Human Histone Deacetylase 8*

Cell Morphology of Differentiated SH-SY5Y Cells

Undifferentiated SH-SY5Y cells (day 0) showed a rounded morphology with limited neurite outgrowth and formed compact cell clusters. After exposure to ATRA for 3 days, cells began to extend short neurite-like processes and displayed a more elongated cell body, indicating the onset of neuronal differentiation. By day 5, the majority of cells exhibited a pronounced neuron-like morphology, characterized by slender, branched neurites and interconnected networks, confirming successful differentiation into a more mature neuronal phenotype (Figure 6: panels for day 0, day 3, and day 5).

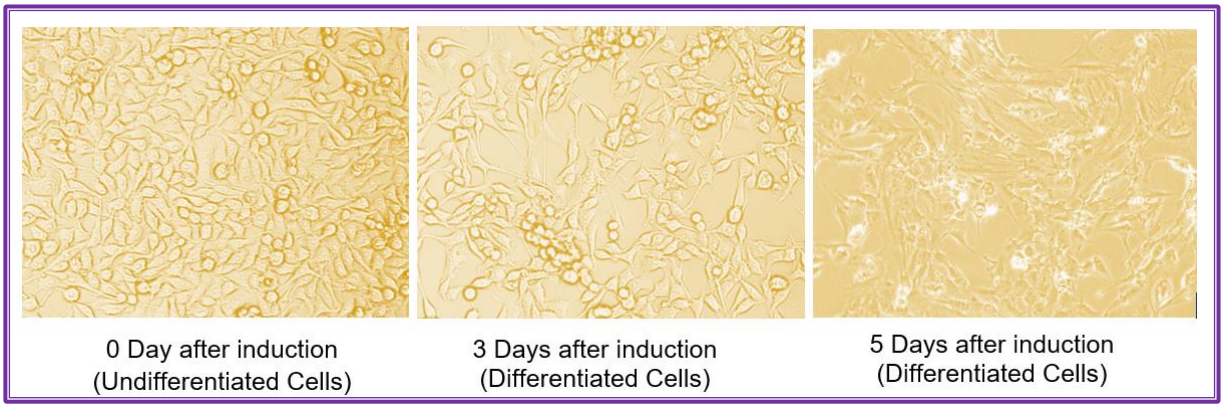


Figure 6*: Morphological Changes in SH-SY5Y Cells During ATRA-Induced Differentiation*

Effect of Phlorizin on SH-SY5Y Cell Morphology

ATRA maintained typical neuron-like morphology, with intact cell bodies and well-defined neuritic networks. Treatment with PZ at 2.5 and 5µg/mL did not produce obvious morphological alterations compared to the control, and cells largely retained normal neurite length and branching. At higher concentrations (10-40 µg/mL), cell density gradually decreased, accompanied by shortening and partial retraction of neurites, with some cells appearing shrunken and rounded at the highest dose (40 µg/mL) (Figure 7: control, 2.5, 5, 10, 20, 40 µg/mL). These changes are consistent with a concentration-dependent cytotoxic effect of PZ on differentiated SH-SY5Y cells.

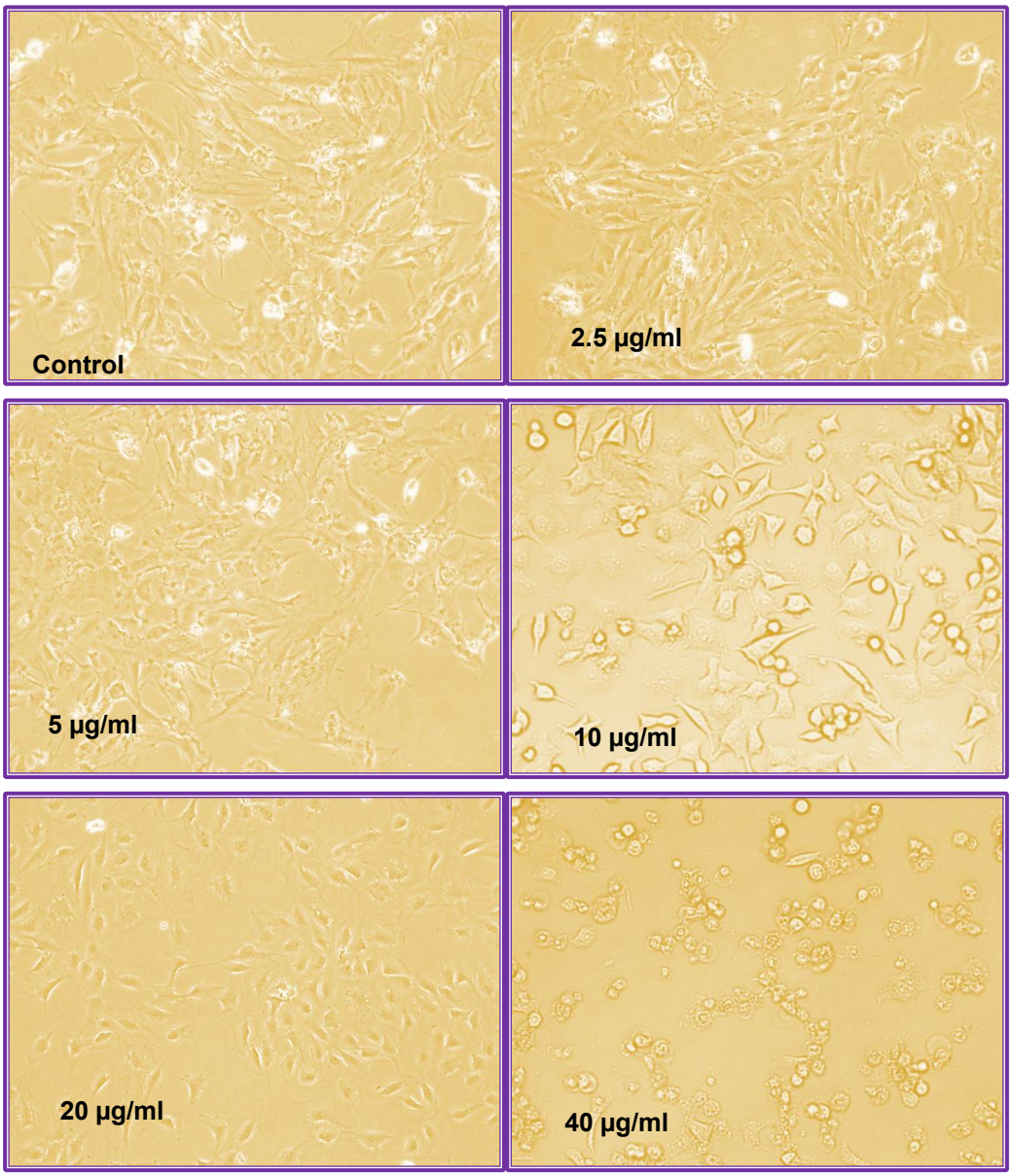


Figure 7: *Effect Of Phlorizin on the Morphology of ATRA-Differentiated SH-SY5Y Cells*

Effect of Phlorizin on SH-SY5Y cell viability (MTT assay)

The MTT assay showed that PZ reduced the viability of ATRA-differentiated SH-SY5Y cells in a clear concentration-dependent manner, as illustrated by the dose-response curve in Figure 8. Untreated control cells were taken as 100% viable. At 2.5, 5, 10, 20 and 40 µg/mL of PZ, the mean cell viabilities were 84.49 ± 1.82%, 75.83 ± 0.45%, 44.55 ± 0.96%, 23.66 ± 1.01% and 8.09 ± 0.52%, respectively (mean ± SD, n = 3) as summarized in Figure 9. This pattern indicates a gradual shift from modest cytotoxicity at low concentrations to almost complete loss of viable cells at the highest concentration tested.

When expressed as percentage cytotoxicity, PZ produced 15.51 ± 1.82%, 24.17 ± 0.45%, 55.45 ± 0.96%, 76.34 ± 1.01%, and 91.91 ± 0.52% cytotoxicity. Non-linear regression analysis of the dose-response curve (figure 8) yielded an IC_{50} value of 9.13 µg/mL for PZ in differentiated SH-SY5Y cells. Statistically significant reductions in viability were observed from 10 µg/mL onwards compared with control ($p < 0.05$), confirming that PZ exerts a strong dose-dependent cytotoxic effect on neuron-like SH-SY5Y cells.

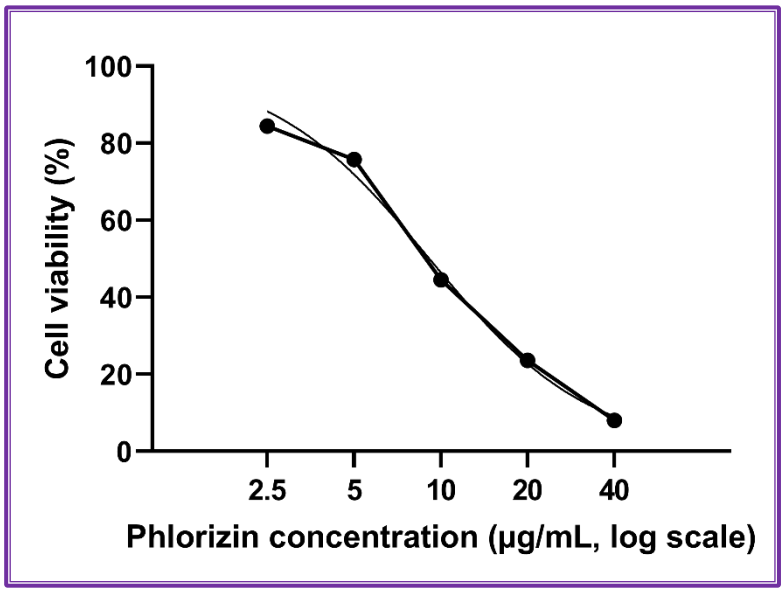


Figure 8: *Dose-Response Curve Showing the Effect of Phlorizin on % Cell Viability of ATRA-Differentiated SH-SY5Y Cells*

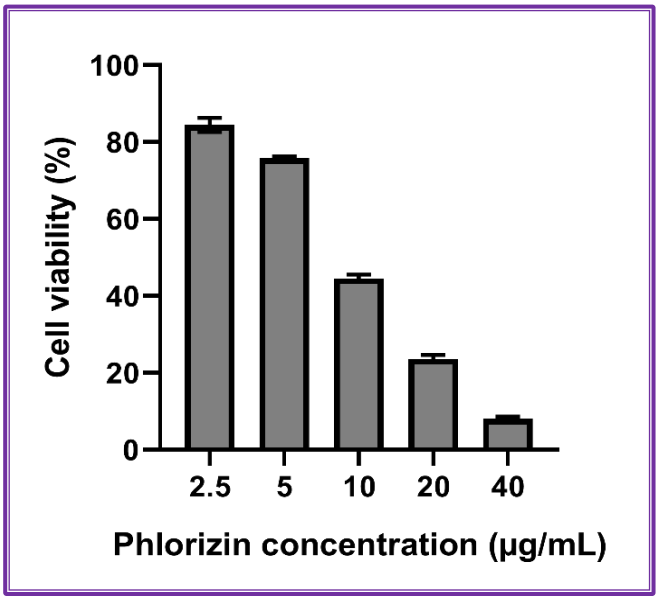


Figure 9: *Effect of Increasing Phlorizin Concentrations On % Cell Viability of ATRA-Differentiated SH-SY5Y Cells*

Discussion

This work shows that PZ can be cleanly isolated from *B. blakeana* leaves and that the compound itself is responsible for the biological effects observed in the cell and docking studies. The chromatography profile, single TLC spot, and consistent spectroscopic data (MS, ^{1}H-NMR, ^{13}C-NMR, FT-IR) all point to a well-defined molecule rather than a mixture, so the downstream findings can be attributed with confidence to PZ and not to unknown contaminants. Establishing *B. blakeana* as a source of this dihydrochalcone also broadens the list of PZ-containing plants and may be useful for future phytochemical or pharmacological work (Shalom *et al*., 2025). Plant derived phenolics and other secondary metabolites are widely evaluated for antioxidant, antimicrobial and anticancer activity and under-explored plant sources continue to be screened for such compounds (Ozkan *et al*., 2026).

The spectral characterization confirms that the isolated compound is identical to PZ, as described in earlier phytochemical reports, with a matching molecular mass, diagnostic aromatic and sugar proton signals, and characteristic carbonyl and glycosidic carbon resonances (Perumal *et al.,* 2023). Prior

studies on PZ and related dihydrochalcones have mainly focused on their roles as SGLT inhibitors and antioxidants (Batra *et al*., 2023; Ni *et al*., 2024), showing that the same molecule in *B. blakeana* helps connect the findings to that wider literature without introducing a new, uncharacterized entity.

The docking analysis suggests that PZ can occupy the catalytic pocket of HDAC8 with a plausible binding pose and moderate affinity(Bora-Tatar *et al.*, 2009). The predicted binding energy and low-micromolar inhibition constant are within the range reported for weaker natural HDAC ligands, and the network of hydrogen bonds with His143, His180 and Gly206, supported by contacts with residues such as Asp101, Phe207 and Tyr306, is consistent with binding near the Zn^{2+}-containing active site (Uba & Zengin, 2023, Dwivedi *et al*., 2026).

In the differentiated SH-SY5Y model, PZ clearly behaves as a concentration-dependent cytotoxin rather than a simple neuroprotective agent. Morphological changes—loss of neuritic networks, cell body shrinkage, and rounding at higher doses, track closely with the MTT data, where viability falls from around 80-85% at 2.5-5 µg/mL to below 10% at 40 µg/mL. The IC_{50} value near 9 µg/mL places PZ among phenolic compounds of moderate potency in neuronal cell lines and is comparable to doses where other polyphenols shift from protective to damaging effects. Taken together, these observations support a hermetic pattern: low concentrations are relatively well tolerated, whereas higher concentrations become overtly harmful to neuron-like cells (Perrone & D'Angelo, 2025; Son *et al.,* 2008).

These findings also fit into a broader and sometimes contradictory body of work on PZ. In several systems, PZ and related dihydrochalcones have been described as antioxidants or neuroprotectants(Tian *et al*., 2021), particularly when used at lower concentrations or under oxidative or amyloid-β stress. A crude ethanolic leaf extract of *Bauhinia thailandica* reduced ROS, nitric oxide, and pro-inflammatory cytokines in LPS-stimulated BV2 microglia at 12.5–25 µg/mL, which is consistent with a protective effect under inflammatory stress, albeit the active ingredients were not identified (Promprom *et al*., 2026). In contrast, our study examines basal conditions and shows that, in the absence of an external insult, PZ can itself drive loss of neuronal viability when the dose is sufficiently high. This dual behaviour is common among polyphenols and highlights that any therapeutic use of PZ would require careful control of concentration, exposure time and disease context to avoid tipping from protective signalling into cytotoxicity (Galati & O'Brien, 2004; Jalouli *et al.,* 2025, Sakihama*et al.,* 2002).

Limitations

The docking analysis is purely computational, relying on a single static HDAC8 crystal structure, and was not backed by re-docking controls, molecular dynamics, or cell-free enzymatic assays, so the predicted binding has not been verified biochemically. The in vitro data come from a single neuron-like cell line using one retinoic acid differentiation protocol and were assessed only by MTT viability, which does not provide information on apoptosis, oxidative stress, mitochondrial dysfunction, or intracellular HDAC activity. In addition, no in vivo or pharmacokinetic data exist to support the translation of the concentrations evaluated.

Future Scope

Docking should be extended to other HDAC isoforms and targets, with molecular dynamics and re-docking controls to evaluate selectivity, and combined with cell-free HDAC assays to confirm that binding translates into inhibition (Shen & Kozikowski, 2016). Because loss of viability was observed at higher doses, apoptosis markers, ROS assays, and mitochondrial membrane potential measurements could clarify the underlying mechanism. PZ should also be tested in other neuronal and glial models, or in vivo, under Alzheimer's-relevant stress such as amyloid-β exposure, to determine whether its basal cytotoxicity can shift toward protection and whether a therapeutic window can be established.

Conclusion

This study shows that *Bauhinia blakeana* leaves are a reliable source of phlorizin and that the isolated compound was structurally identical to PZ reported from other plants. Computational docking suggests that phlorizin can occupy the catalytic pocket of HDAC8 in a reasonable binding orientation, pointing to a potential interaction with epigenetic machinery. In differentiated SH-SY5Y cells, phlorizin produced a clear, concentration-dependent loss of viability that matched the observed morphological damage. Taken together, these findings position *B. blakeana*-derived phlorizin as a well-characterised natural molecule with measurable effects on a neuronal model and a plausible link to HDAC8. The next steps should include direct enzyme assays to confirm HDAC inhibition, broader target profiling, and studies in additional neuronal and glial systems, ideally under disease-relevant stress conditions.

Conflict of Interest

The authors declare no conflict of interest

Acknowledgement

The authors thank Karpagam Academy of Higher Education, Coimbatore, for providing the facilities and institutional support needed to carry out this work. The authors are grateful to the Ministry of Environment, Forest & Climate Change, Government of India, for the authentication of *Bauhinia blakeana.*

References

Banerjee, S., Adhikari, N., Amin, S. A., & Jha, T. (2019). Histone deacetylase 8 (HDAC8) and its inhibitors with selectivity to other isoforms: An overview. *European Journal of Medicinal Chemistry*, *164*, 214-240.https://doi.org/10.1016/j.ejmech.2018.12.039

Batra, S., Bamrah, P. K., & Choudhary, M. (2023). Sodium-glucose transporter (SGLT2) inhibition: A potential target for treatment of type-2 Diabetes Mellitus with Natural and Synthetic compounds. *Egyptian Journal of Basic and Applied Sciences*, *10*(1), 69-82. https://doi.org/10.1080/2314808X.2022.2145734

Bora-Tatar, G., Dayangaç-Erden, D., Demir, A. S., Dalkara, S., Yelekçi, K., & Erdem-Yurter, H. (2009). Molecular modifications on carboxylic acid derivatives as potent histone deacetylase inhibitors: Activity and docking studies. *Bioorganic & Medicinal Chemistry*, *17*(14), 5219-5228. https://doi.org/10.1016/j.bmc.2009.05.042

Cavalli, A., Bolognesi, M. L., Minarini, A., Rosini, M., Tumiatti, V., Recanatini, M., & Melchiorre, C. (2008). Multi-target-directed ligands to combat neurodegenerative diseases. *Journal of Medicinal Chemistry*, *51*(3), 347-372. https://doi.org/10.1021/jm7009364

Cheung, Y. T., Lau, W. K. W., Yu, M. S., Lai, C. S. W., Yeung, S. C., So, K. F., & Chang, R. C. C. (2009). Effects of all-trans-retinoic acid on human SH-SY5Y neuroblastoma as in vitro model in neurotoxicity research. *Neurotoxicology*, *30*(1), 127-135. https://doi.org/10.1016/j.neuro.2008.11.001

Chhimwal, J., Goel, A., Sukapaka, M., Patial, V., & Padwad, Y. (2022). Phloretin mitigates oxidative injury, inflammation, and fibrogenic responses via restoration of autophagic flux in in vitro and preclinical models of NAFLD. *The Journal of Nutritional Biochemistry*, *107*, 109062. https://doi.org/10.1016/j.jnutbio.2022.109062

Dwivedi, P. S., Mole, S. S., & Shastry, C. S. (2026). The neuroprotective potential of diosgenin: an integrated in silico, in vitro, and in vivo approach in colchicine-induced Alzheimer's model. *Journal of Computer-Aided Molecular Design*, *40*(1), 115. https://doi.org/10.1007/s10822-026-00819-0

Ehrenkranz, J. R., Lewis, N. G., Ronald Kahn, C., & Roth, J. (2005). Phlorizin: A review. *Diabetes/metabolism Research and Reviews*, *21*(1), 31-38. https://doi.org/10.1002/dmrr.532

Encinas, M., Iglesias, M., Liu, Y., Wang, H., Muhaisen, A., Cena, V., ... & Comella, J. X. (2000). Sequential treatment of SH-SY5Y cells with retinoic acid and brain-derived neurotrophic factor gives rise to fully differentiated, neurotrophic factor-dependent, human neuron-like cells. *Journal of Neurochemistry*, *75*(3), 991-1003. https://doi.org/10.1046/j.1471-4159.2000.0750991.x

Galati, G., &O'brien, P. J. (2004). Potential toxicity of flavonoids and other dietary phenolics: significance for their chemopreventive and anticancer properties. *Free radical biology and medicine*, *37*(3), 287-303. https://doi.org/10.1016/j.freeradbiomed.2004.04.034

Gosch, C., Halbwirth, H., & Stich, K. (2010). Phloridzin: Biosynthesis, distribution and physiological relevance in plants. *Phytochemistry*, *71*(8-9), 838-843. https://doi.org/10.1016/j.phytochem.2010.03.003

Hanwell, M. D., Curtis, D. E., Lonie, D. C., Vandermeersch, T., Zurek, E., & Hutchison, G. R. (2012). Avogadro: an advanced semantic chemical editor, visualization, and analysis platform. *Journal of Cheminformatics*, *4*(1), 17. https://doi.org/10.1186/1758-2946-4-17

Jalouli, M., Rahman, M. A., Biswas, P., Rahman, H., Harrath, A. H., Lee, I. S., ... & Kim, B. (2025). Targeting natural antioxidant polyphenols to protect neuroinflammation and neurodegenerative diseases: A comprehensive review. *Frontiers in Pharmacology*, *16*, 1492517. https://doi.org/10.3389/fphar.2025.1492517

Kim, S., Chen, J., Cheng, T., Gindulyte, A., He, J., He, S., ... & Bolton, E. E. (2021). PubChem in 2021: New data content and improved web interfaces. *Nucleic Acids Research*, *49*(D1), D1388-D1395. https://doi.org/10.1093/nar/gkaa971

Long, J. M., & Holtzman, D. M. (2019). Alzheimer disease: an update on pathobiology and treatment strategies. *Cell*, *179*(2), 312-339. https://doi.org/10.1016/j.cell.2019.09.001

Morris, G. M., Huey, R., Lindstrom, W., Sanner, M. F., Belew, R. K., Goodsell, D. S., & Olson, A. J. (2009). AutoDock4 and AutoDockTools4: Automated docking with selective receptor flexibility. *Journal of Computational Chemistry*, *30*(16), 2785-2791. https://doi.org/10.1002/jcc.21256

Mosmann, T. (1983). Rapid colorimetric assay for cellular growth and survival: Application to proliferation and cytotoxicity assays. *Journal of Immunological Methods*, *65*(1-2), 55-63. https://doi.org/10.1016/0022-1759(83)90303-4

Najafian, M., Jahromi, M. Z., Nowroznejhad, M. J., Khajeaian, P., Kargar, M. M., Sadeghi, M., & Arasteh, A. (2012). Phloridzin reduces blood glucose levels and improves lipids metabolism in streptozotocin-induced diabetic rats. *Molecular Biology Reports*, *39*(5), 5299-5306. https://doi.org/10.1007/s11033-011-1328-7

Ni, T., Zhang, S., Rao, J., Zhao, J., Huang, H., Liu, Y., ... & Sun, Y. (2024). Phlorizin, an important glucoside: Research progress on its biological activity and mechanism. *Molecules*, *29*(3), 741. https://doi.org/10.3390/molecules29030741

Ozkan, A. I., Yüce, K., & Aslan, N. (2026). Biological Effects and Phytochemical Composition of Wild Food Plants (WFPs) in Alpine Zones. In *Conservation, Climate, and Sustainable Use in Alpine Ecosystems* (pp. 279-340). IGI Global Scientific Publishing. https://doi.org/10.4018/979-8-2600-1207-9.ch011

Perrone, P., & D'Angelo, S. (2025). Hormesis and health: molecular mechanisms and the key role of polyphenols. *Food Chemistry Advances*, *7*, 101030. https://doi.org/10.1016/j.focha.2025.101030

Perumal, P., Arthanari, U., &Sanniyasi, E. (2023). Phlorizin isolated from seagrass Syringodiumisoetifolium inhibits diethylnitrosamine and carbon tetrachloride-induced hepatocellular carcinoma in BALB/c mice. *South African Journal of Botany*, *155*, 1-15. https://doi.org/10.1016/j.sajb.2023.02.002

Promprom, W., Chatan, W., Homwutthiwong, K., Apaijit, K., Cheepsunthorn, P., &Mairuae, N. (2026). Anti-Inflammatory and Antioxidant Properties of Bauhinia thailandica Leaf Extract in Microglial Cells. *International Journal of Molecular Sciences*, *27*(6), 2809. https://doi.org/10.3390/ijms27062809

Rajani, M., & Kanaki, N. S. (2008). Phytochemical Standardization of Herbal Drugs and Polyherbal Formulations. In: Ramawat, K., Merillon, J. (eds) Bioactive Molecules and Medicinal Plants. Springer, Berlin, Heidelberg. https://doi.org/10.1007/978-3-540-74603-4_19

Ribeiro, F. F., Mendonca Junior, F. J., Ghasemi, J. B., Ishiki, H. M., Scotti, M. T., & Scotti, L. (2018). Docking of natural products against neurodegenerative diseases: General concepts. *Combinatorial Chemistry & High Throughput Screening*, *21*(3), 152-160. https://doi.org/10.2174/1386207321666180313130314

Rieg, T., & Vallon, V. (2018). Development of SGLT1 and SGLT2 inhibitors. *Diabetologia*, *61*(10), 2079-2086. https://doi.org/10.1007/s00125-018-4654-7

Sakihama, Y., Cohen, M. F., Grace, S. C., & Yamasaki, H. (2002). Plant phenolic antioxidant and prooxidant activities: Phenolics-induced oxidative damage mediated by metals in plants. *Toxicology*, *177*(1), 67-80. https://doi.org/10.1016/s0300-483x(02)00196-8

Scheltens, P., De Strooper, B., Kivipelto, M., Holstege, H., Chételat, G., Teunissen, C. E., ... & Van der Flier, W. M. (2021). Alzheimer's disease. *The Lancet*, *397*(10284), 1577-1590. https://doi.org/10.1016/S0140-6736(20)32205-4

Shalom, E. O., Faloye, K. O., Adesida, S. A., Adewole, A. H., Olatunji, O. E., Okunribido, B. I., ... &Famuyiwa, S. O. (2025). Flavonoid in All Their Therapeutic Values: An Odyssey into the Phytochemistry and Pharmacology of Naturally Occurring Flavonoid from Genus Bauhinia. *Molecules*, *30*(16), 3335. https://doi.org/10.3390/molecules30163335

Shen, S., & Kozikowski, A. P. (2016). Why hydroxamates may not be the best histone deacetylase inhibitors—what some may have forgotten or would rather forget? *ChemMedChem*, *11*(1), 15-21. https://doi.org/10.1002/cmdc.201500486

Solanki, I., Parihar, P., Mansuri, M. L., & Parihar, M. S. (2015). Flavonoid-based therapies in the early management of neurodegenerative diseases. *Advances in Nutrition*, *6*(1), 64-72. https://doi.org/10.3945/an.114.007500

Son, T. G., Camandola, S., & Mattson, M. P. (2008). Hormetic dietary phytochemicals. *Neuromolecular Medicine*, *10*(4), 236-246. https://doi.org/10.1007/s12017-008-8037-y

Tian, L., Cao, J., Zhao, T., Liu, Y., Khan, A., & Cheng, G. (2021). The bioavailability, extraction, biosynthesis and distribution of natural dihydrochalcone: Phloridzin. *International Journal of Molecular Sciences*, *22*(2), 962. https://doi.org/10.3390/ijms22020962

Trott, O., & Olson, A. J. (2010). AutoDock Vina: improving the speed and accuracy of docking with a new scoring function, efficient optimization, and multithreading. *Journal of Computational Chemistry*, *31*(2), 455-461. https://doi.org/10.1002/jcc.21334

Uba, A. I., & Zengin, G. (2023). Phenolic compounds as histone deacetylase inhibitors: binding propensity and interaction insights from molecular docking and dynamics simulations: AI Uba and G. Zengin. *Amino Acids*, *55*(5), 579-593. https://doi.org/10.1007/s00726-023-03249-6

Vannini, A., Volpari, C., Gallinari, P., Jones, P., Mattu, M., Carfí, A., ... & Di Marco, S. (2007). Substrate binding to histone deacetylases as shown by the crystal structure of the HDAC8–substrate complex. *The EMBO Reports*, *8*(9), 879-884. https://doi.org/10.1038/sj.embor.7401047

Williams, R. J., & Spencer, J. P. (2012). Flavonoids, cognition, and dementia: Actions, mechanisms, and potential therapeutic utility for Alzheimer disease. *Free Radical Biology and Medicine*, *52*(1), 35-45. https://doi.org/10.1016/j.freeradbiomed.2011.09.010

Xicoy, H., Wieringa, B., & Martens, G. J. (2017). The SH-SY5Y cell line in Parkinson's disease research: Asystematic review. *Molecular Neurodegeneration*, *12*(1), 10. https://doi.org/10.1186/s13024-017-0149-0